Immunological characterization of peritoneal exudate cells in liver cirrhosis patients

Authors:

Shiori Kaji, MD[1], Izumi Sasaki, PhD[2,*], Satoko Kunimoto, MD[3], Naoko Wakaki-Nishiyama, BS[2], Emi Tosuji, MD[4], Ayano Kurara, HSG[2], Takashi Kato, MD, PhD[2,5], Chisako Mutsukawa, BS[2], Daisuke Okuzaki, PhD[6], Chizuyo Okamoto, BS[2], Yukiko Yamano, MD[3], Ryo Shimizu, MD[1], Shuya Maeshima, MD[1], Yoshiyuki Ida, MD, PhD[1], Yasunobu Yamashita, MD, PhD[1], Tadamichi Hashimoto, MD, PhD[7], Sadahiro Iwabuchi, PhD[8], Shinichi Hashimoto, PhD[8], Shin-Ichiroh Saitoh, PhD[9], Shin-ichi Araki, MD, PhD[3], Masayuki Kitano, MD, PhD[1,*] and Tsuneyasu Kaisho, MD, PhD[2,*]

Affiliations:

[1] Second Department of Internal Medicine, Wakayama Medical University, Wakayama, Japan.

[2] Department of Immunology, Institute of Advanced Medicine, Wakayama Medical University, Wakayama, Japan.

[3] Department of Nephrology, Wakayama Medical University, Wakayama, Japan.

[4] Department of Dermatology, Wakayama Medical University, Wakayama, Japan.

[5] Department of Rheumatology and Clinical Immunology, Wakayama Medical University, Wakayama, Japan.

[6] Laboratory for Human Immunology (Single Cell Genomics), WPI Immunology Frontier Research Center, Osaka University, Suita-City, Osaka, Japan.

[7] Medical Corporation Hashimoto Hospital, Wakayama, Japan.

[8] Department of Molecular Pathophysiology, Institute of Advanced Medicine, Wakayama Medical

University, Wakayama, Japan.

[9] Department of Intractable Disorders, Institute of Advanced Medicine, Wakayama Medical University, Wakayama, Japan.

Address correspondence:

*Corresponding author. Email: izumisas@wakayama-med.ac.jp (I.S); kitano@wakayama-med.ac.jp (M.K) ; tkaisho@wakayama-med.ac.jp (T.Kai.)

Conflicts of interest: nothing to report.

Financial support: This work was supported in part by 2023 Wakayama Medical Award for Young Researchers (to S.K.). This work was also supported by Grant-in-Aid for Transformative Research Areas (JP22H05182 and JP22H05187 to T. Kai. and JP22H05187 to I.S.), for Scientific Research (B) (JP26293106, JP17H04088, JP20H03505 and JP24K02298 to T. Kai.), for Scientific Research (C) (JP19K07628 and JP22K07006 to I.S.), for Scientific Research on Innovative Areas (JP17H05799 and JP19H04813 to T. Kai.), for Exploratory Research (JP17K19568, JP21K19384 and JP23K18222 to T. Kai.), for Research Activity Start-up (JP23K19487 to T.Kat) from the Japan Society for the Promotion of Science, Takeda Science Foundation (to T. Kai. and I.S.), GSK Japan Research Grant 2021 (to I.S.), Kowa Life Science Foundation (to I.S.).

Keywords: continuous ambulatory peritoneal dialysis, dendritic cells, GATA6-expressing macrophages, mucosal-associated invariant T cells, Child-Pugh classification

Abbreviations: LC, liver cirrhosis; MAIT cells, mucosal-associated invariant T cells; PECs,

peritoneal exudate cells; CAPD, continuous ambulatory peritoneal dialysis; DCs, dendritic cells; scRNA-seq, single-cell RNA sequencing; UMAP, Uniform Manifold Approximation and Projection; KEGG, Kyoto Encyclopedia of Genes and Genomes; CP-B, Child-Pugh class B; bulk RNA-seq, bulk RNA sequencing; CP, Child-Pugh; CP-C, Child-Pugh class C; *GATA6*$^{+}$ MPs, *GATA6*-expressing macrophages; *FCGR3A*$^{+}$ MPs, *FCGR3A*-expressing macrophages.

ABSTRACT

BACKGROUND AND AIMS: Liver cirrhosis (LC) is the end stage of liver fibrosis caused by various chronic liver diseases. Patients with LC often develop ascites containing peritoneal exudate cells (PECs). However, those cells have not been fully immunologically characterized. In this study, we clarify immune cell profiles of PECs from patients with LC.

APPROACH AND RESULTS: PECs were collected from patients with LC or patients receiving continuous ambulatory peritoneal dialysis (CAPD) as a non-cirrhotic control and subjected to single-cell RNA sequencing (scRNA-seq), bulk RNA sequencing (RNA-seq) and flowcytometry analyses. Analysis of scRNA-seq revealed that dendritic cells (DCs) and macrophages were major populations in CAPD patient-derived PECs, while those cells were decreased and T cells were most abundant in LC patient-derived PECs. Notably, *FCGR3A*-expressing macrophages were dominant over DCs and *GATA6*-expressing macrophages in LC patient-derived PECs. Bulk RNA-seq analysis further clarified expression of a set of genes was up- or down-regulated along with LC severity. Especially, expression of T cell signature genes was featured by its increase at Child-Pugh class B, but decrease at Child-Pugh class C. Flowcytometry analysis showed increase of T cells, decrease of DCs and macrophages, and increased expression of CD16 and CD163 in $CD1c^{int}CD14^{high}$ cells corresponding to *FCGR3A*-expressing macrophages in LC patient-derived PECs.

CONCLUSIONS: In LC patient-derived PECs, myeloid and T cell populations and their gene expression profiles were fluctuated with severity. Our findings should contribute to further development of diagnosis or therapeutic maneuver for LC.

INTRODUCTION

Liver cirrhosis (LC) is an end stage of liver fibrosis and causes more than one million deaths

every year all over the world.[1] As liver fibrosis progresses, patients often develop ascites, mainly due to portal hypertension. A variety of immune cells can be found in the ascites and they change their profiles, depending on the pathological state of the patients. For example, in patients with LC, $CD8^+$ mucosal-associated invariant T (MAIT) cells and $CD16^{high}$ $CD163^{high}$ macrophages are increased in the ascites but not in peripheral bloods.[2] In mice, peritoneal cavity macrophages migrate into the liver upon liver injury,[3] and regulate the pathological conditions in the liver.[4,5] These studies indicate peritoneal cavity cells should have critical roles in liver pathogenesis. However, it is unclear whether or how various types of immune cells fluctuate in the ascites of patients with LC.

In this study, we analyzed the peritoneal exudate cells (PECs) of patients with LC in comparison with those of patients undergoing continuous ambulatory peritoneal dialysis (CAPD). We then found increase in frequency of T cells and macrophage subsets and decrease in frequency of dendritic cells (DCs) in the ascites of LC patients. Furthermore, we have also revealed some parameters correlating with disease severity.

MATERIALS AND METHODS

Patients

Patients with LC and patients with end-stage renal disease undergoing CAPD at Wakayama Medical University were eligible for this study (Supplementary Table S1-3). Written informed consent was obtained from all patients, and the study protocol conforms to the ethical guidelines of the 2013 Declaration of Helsinki and the 2018 Declaration of Istanbul. All studies were performed in accordance with appropriate ethical regulations and were pre-approved by the Wakayama Medical University Research Ethics Committee (#3918).

104 **Preparation of peritoneal exudate cells**

105 PECs from patients with LC were collected from ascites by puncture and drainage at the
106 diagnosis or treatment. PECs from patients undergoing CAPD were collected from 1.5-2 L of
107 CAPD effluent according to the standard CAPD prescription. Ascites of patients with LC or
108 CAPD effluent were centrifuged at 4°C 2000 rpm 5 min. Cell pellets were washed three times
109 with phosphate buffered saline (PBS) and resuspended in PBS supplemented with 1% fetal calf
110 serum (FCS), 5 mM ethylenediaminetetraacetic acid (EDTA) and 0.01% sodium azide (NaN_3).
111 Turk's solution was used to analyze cell viability to ensure single-cell suspension with more
112 than 90% viability.

113

114 **Single-cell RNA sequencing analysis**

115 Single-cell RNA sequencing (scRNA-seq) analysis was performed using Chromium Controller
116 (10x Genomics, Pleasanton, CA). Libraries were sequenced on NovaSeq 6000 (Illumina, San
117 Diego, CA) in a 101+101 base paired-end mode. Illumina RTA v3.4.4 software was used for
118 base calling. Generated reads were input into the cellranger pipeline (cellranger-7.1.0, 10x
119 Genomics) for UMI counting for each gene-cell (barcode) combination. The cluster analysis
120 based on Uniform Manifold Approximation and Projection (UMAP) plot and differential
121 expression analysis were performed by Loupe Browser (v7.0.1, 10x Genomics).

122

123 **Bulk RNA sequencing analysis**

124 Total RNA was extracted with RNeasy micro kit (QIAGEN, Hilden, Germany). Full-length
125 cDNA was prepared using a SMART-Seq HT Kit (Takara Bio, Japan). According to the
126 SMART-Seq kit instructions, an Illumina library was then prepared using a NexteraXT DNA
127 Library Preparation Kit (Illumina). Sequencing was performed on NovaSeq 6000 platform in a

128 101-base single-end mode. Illumina RTA v3.4.4 software was used for base calling. Generated
129 reads were mapped to the human (hg19) reference genome using TopHat v2.1.1 in combination
130 with Bowtie2 ver. 2.2.8 and SAMtools ver. 0.1.18. Fragments per kilobase of exon per million
131 mapped fragments (FPKMs) were calculated using Cuffdiff 2.2.1 with parameter -max-bundle-
132 frags 50000000. The DAVID Bioinformatics database and Kyoto Encyclopedia of Genes and
133 Genomes (KEGG) annotations were used for enrichment analysis. The web tools ClustVis and
134 VolcaNoseR[6] were used to draw heatmaps and volcano plots, respectively.
135
136 **Flowcytometry analysis**
137 PECs were collected in Eppendorf tubes from patients undergoing CAPD or patients with LC,
138 and subjected to flowcytometry analysis. PECs were stained with the antibodies listed in
139 Supplementary Table S4. Dead cells detected as positive for AmCyan channels were excluded
140 using the LIVE/DEAD Fixable Dead Cell Aqua Stain Kit (cat; L34966, Invitrogen, Waltham,
141 MA). Stained cells were analyzed with FACS Verse and data were processed with FlowJo
142 Version 10.8.1 software (TreeStar, Ashland, OR).
143
144 **Magnetic beads cell isolation**
145 $CD1c^{high}$ $CD14^{int}$, $CD1c^{int}$ $CD14^{high}$ or $CD1c^{low\text{-}int}$ $CD14^{low}$ cells were isolated from PECs by
146 using magnetic-activated cell sorting (MACS). PECs were stained with biotinylated anti-CD1c
147 antibody for 20 min on ice. After washing, stained PECs were applied to streptavidin microbeads
148 (Miltenyi Biotec, Bergisch Gladbach, Germany) and then magnetically sorted with LS columns
149 as per the manufacturer's instructions. Streptavidin microbeads-conjugated cells were used as
150 $CD1c^{high}$ $CD14^{int}$ cells. The flow-through cells including $CD1c^{int}$ $CD14^{high}$ and $CD1c^{low\text{-}int}$ $CD14^{low}$
151 cells were stained with PE-conjugated anti-CD14 antibody for 20 min on ice. After washing, cells

152 were applied to PE microbeads (Miltenyvi Biotec) and then magnetically sorted with LS columns
153 as per the manufacturer's instructions. PE microbeads-conjugated cells were used as $CD1c^{int}$
154 $CD14^{high}$ cells and the flow-through cells were used as $CD1c^{low\text{-}int}$ $CD14^{low}$ cells. Purity of
155 $CD1c^{high}$ $CD14^{int}$, $CD1c^{int}$ $CD14^{high}$ or $CD1c^{low\text{-}int}$ $CD14^{low}$ cells were verified by flowcytometry
156 analysis.
157
158 **Quantitative real-time PCR**
159 Using PrimeScript RT Reagent Kit (TaKaRa, Kusatsu, Japan), 0.5 μg of total RNA was reverse
160 transcribed into complementary DNA. Relative expression of RNA transcripts was quantified
161 using gene-specific primers, TB Green Premix Ex Taq II (TaKaRa) and the StepOnePlus Real-
162 Time PCR System (Applied Biosystems, Waltham, MA). TaqMan probes (TaqMan Gene
163 Expression Assay, Applied Biosystems) were used for 18S rRNA (internal control). Expression
164 of all genes was normalized to that of 18S rRNA and is represented as the ratio to the indicated
165 reference samples. Gene-specific primers used in the study were obtained from FASMAC, and
166 all primers were validated for linear amplification. The primer sequences were designed and
167 synthesized by FASMAC as follows: *GATA6*, forward primer: 5'-
168 GCCACTACCTGTGCAACGCCT-3', reverse primer: 5'-CAATCCAAGCCGCCGTGATGAA-
169 3'.
170
171 **Statistical analysis**
172 Statistical significance was determined by an unpaired two-tailed Student's t test. p values are
173 indicated by $*p < 0.05$, $**p < 0.01$, $***p < 0.001$, $****p < 0.0001$. $p < 0.05$ was considered
174 statistically significant.
175

176 **Data availability statement**

177 Bulk RNA sequencing (bulk RNA-seq) and scRNA-seq data generated in this study have been
178 deposited at GEO under accession number GSE287363 and GSE287364, respectively.

179

180 **RESULTS**

181 **Single-cell RNA-seq analysis of LC and CAPD patient-derived PECs**

182 We first collected PECs from a patient with LC at Child-Pugh class B (CP-B) and from a
183 patient undergoing CAPD on the same day and performed scRNA-seq analysis (Fig. 1A).
184 According to several signature genes, five cell clusters including T cells, B cells, *GATA6*-
185 expressing macrophages, DCs and *FCGR3A*-expressing macrophages were defined (Fig. 1B,C).
186 In CAPD patient-derived PECs, the frequencies of T cells, B cells, *GATA6*-expressing
187 macrophages, DCs and *FCGR3A*-expressing macrophages were 18%, 1.4%, 9.8%, 30% and
188 40%, respectively. DCs and macrophages occupied around 80% of total PECs. In LC patient-
189 derived PECs, T cells were significantly increased to 73% and became the most abundant
190 population. Meanwhile, *GATA6*-expressing macrophages, DCs and *FCGR3A*-expressing
191 macrophages were decreased to 1.6%, 2.1% and 16%, respectively. Due to the most prominent
192 decrease of DCs, *FCGR3A*-expressing macrophages were dominant over *GATA6*-expressing
193 macrophages and DCs in LC patient-derived PECs.

194 We then investigated expression of DC signature genes. According to the heatmap, feature plot
195 and violin plot analyses, expression of DC signature genes, including CD1 family members
196 (*CD1A, CD1B, CD1C, CD1D, CD1E*), *FLT3*, *FCER1A* and HLA family gene (*HLA-DRA*), were
197 much lower in DCs of LC patient-derived PECs than in DCs of CAPD patient-derived PECs
198 (Fig. 1C,D).

199 *FCGR3A*-expressing macrophages are featured by expression of *CD163*, *MARCO*, *SIGLEC1*
200 and *LYVE1*, and this type of macrophage has been reported to be involved in tissue repair.[7]

201 *CD163*, *MARCO*, *SIGLEC1* and *LYVE1* were expressed in *FCGR3A*-expressing macrophages in
202 CAPD patient-derived PECs (Fig. 1C,E). Expression levels of these genes was increased in LC
203 patient-derived PECs.
204 In mice, macrophages expressing a transcription factor, GATA6, occupy around 90% of
205 resident peritoneal macrophages.[8-10] GATA6 is essential for generation of resident peritoneal
206 macrophages and its target genes include *Serpinb2*, *Nt5e*, *Itga6*, *Thbs1*, *Tgfb2*, *Ltbp1*[10] and
207 *CD9*.[9] *GATA6*-expressing macrophages also exist in humans, although they represent less than
208 10% and are not a major population.[11] *CD9*, *SERPINB2, NT5E, ITGA6, THBS1, TGFB2* and
209 *LTBP1* were highly expressed in *GATA6*-expressing macrophages in CAPD patient-derived
210 PECs (Fig. 2A-C). Expression levels of all of these genes except *CD9* and *NT5E* were
211 decreased, while *CD9* and *NT5E* expression was increased in LC patient-derived PECs.
212 *PDGFRB*, *KRT5*, *ACTA2*, *COL1A1* and *UPK3B* were expressed in peritoneal mesothelial cells
213 and classified as peritoneal mesothelial cell signature genes.[12] All of these genes were expressed
214 selectively in *GATA6*-expressing macrophages in CAPD patient-derived PECs (Fig. 2D-F).
215 Furthermore, among them, *PDGFRB*, *KRT5*, *ACTA2*, *COL1A1* and *UPK3B* were expressed at
216 higher levels in LC than in CAPD patient-derived PECs.
217 We then analyzed T cell populations. In LC patient-derived PECs, T cell percentages among
218 PECs were increased and $CD8A^+$ T cells dominated over $CD4^+$ T cells, but the ratio of $CD4^+$ to
219 $CD8A^+$ T cells were not so different from that of CAPD patient-derived PECs (Fig. 3A-C). In
220 both LC and CAPD patient-derived PECs, $CD8A^+$ T cells included a significant fraction of cells
221 expressing *CD8A*, *TRAV1-2* (encoding TCR Vα7.2) and *KLRB1* (encoding CD161), which
222 represent MAIT cells.
223

224 **Bulk RNA-seq analysis revealed down- or up- regulated genes in LC patient-derived PECs**

225 We also performed bulk RNA-seq analysis in PECs from patients with LC and patients
226 undergoing CAPD (Fig. 4A). In comparison to PECs from patients undergoing CAPD,
227 expression of 1107 and 906 genes were more than 2-fold down- and up-regulated, respectively,
228 with significance in PECs from patients with LC (Fig. 4B). The top five downregulated genes in
229 PECs from patients with LC included DC signature genes, such as *CD1C*, *CD1E*, *CD1B* and
230 *FCER1A* (Fig. 4C).

231 KEGG pathway analysis of the top 100 downregulated genes in PECs from patients with LC
232 showed that 'Hematopoietic cell lineage' was the most enriched pathway (Fig. 4D). The
233 pathway contained CD1 family genes (*CD1A*, *CD1B*, *CD1C* and *CD1E*) and *FLT3*, *IL1R2* and
234 *HLA-DQR2*, all of which are dominantly expressed in DCs (Supplementary Figure 1A,B).
235 These CD1 family genes (*CD1A*, *CD1B*, *CD1C* and *CD1E*), *IL1R2* and *LAMC2* were also
236 contained in the second enriched pathway, 'Amoebiasis'. The third enriched pathway
237 was 'ECM-receptor interaction' pathway, which contained *TNC*, *NPNT*, *COL6A3* and *THBS1*.
238 Among the four genes, *TNC*, *NPNT* and *COL6A3* were dominantly expressed in *GATA6*-
239 expressing macrophages and *THBS1* was expressed in DCs and *GATA6*-expressing
240 macrophages. According to the scRNA-seq analysis, we categorized the top 100 downregulated
241 genes in PECs from patients with LC. 82 genes were expressed in DCs or *GATA6*-expressing
242 macrophages. Among them, 37 genes were expressed in both DCs and *GATA6*-expressing
243 macrophages. 45 genes were dominantly expressed in *GATA6*-expressing macrophages, while
244 no genes were expressed dominantly in DCs (shown in light blue in Fig. 4C). Thus, the gene
245 expression analysis indicates that DCs and *GATA6*-expressing macrophages mainly decreased in
246 PECs from patients with LC.

247 KEGG pathway analysis of 100 upregulated genes in PECs from patients with LC

248 showed ’Graft-versus-host disease’ was the most enriched pathway (Fig.4E, F). This pathway
249 contained *GZMB*, *KIR3DL1*, *FASLG*, *KIR3DL2* and *KIR2DL3*, which are highly expressed in T
250 cells (Supplementary Figure 1C,D). Among 100 upregulated genes, 24 genes were dominantly
251 expressed in *FCGR3A*-expressing macrophages (shown in green in Fig. 4E). Those genes
252 include complement genes such as *C1QB*, *C1QC* and *C2*, which belong to the ’Alcoholic liver
253 disease’ pathway. They also include *ABCA1*, *APOE* and *PLTP*, which belong to the ‘Cholesterol
254 metabolism’ pathway. *C1QB*, *C1QC*, *C2*, *ABCA1*, *APOE* and *PLTP* were highly expressed in
255 *FCGR3A*-expressing macrophages in PECs from patients with LC (Supplementary Figure
256 1C,D). These results indicate that T cells and *FCGR3A*-expressing macrophages were increased
257 in PECs from patients with LC.
258
259 **Comprehensive gene expression analysis in correlation with LC severity**
260 We then performed comprehensive gene expression analysis in correlation with LC severity
261 (Fig. 5A, left). Severity of LC was assessed by Child-Pugh (CP) classification, which are widely
262 used.[13] Among eight patients with LC, four patients, including a patient subjected to scRNA-seq
263 analysis, were CP-B and the other 4 patients were Child-Pugh class C (CP-C).
264 We first searched the genes, expression of which decreased with disease severity. Expression
265 of 956 genes were more than 2-fold downregulated in PECs from patients with LC CP-B,
266 compared with PECs from patients undergoing CAPD (Fig.5A, middle). Expression of 443
267 genes were more than 2-fold downregulated in PECs from LC CP-C patients, compared with
268 PECs from patients with LC CP-B (Fig.5A, right). Comparison of these genes revealed that
269 expression of six genes (*CTLA4, C15orf48, PMAIP1, FAM86HP, TNNT1,* and *EPC1*) was
270 decreased as LC gets worse (Fig. 5B,C). Among these genes, *CTLA4, C15orf48, PMAIP1* and

271 *EPC1* were highly expressed in DCs and *GATA6*-expressing macrophages, while *TNNT1* was
272 highly expressed in DCs and *FCGR3A*-expressing macrophages (Supplementary Figure 2A,B).
273 We then searched the genes, the expression of which increased with disease severity.
274 Expression of 1045 genes were more than 2-fold upregulated in PECs from patients with LC
275 CP-B, compared with PECs from patients undergoing CAPD (Fig.5A, middle). Expression of
276 295 genes were more than 2-fold upregulated in PECs from patients with LC CP-C, compared
277 with PECs from patients with LC CP-B (Fig.5A, right). Comparison of these genes clarified that
278 expression of four genes (*IDH1, CMKLR1, SLC7A8* and *SLC46A1*) was increased as LC
279 becomes more severe (Fig.5D, E). All four of these genes were highly expressed in *GATA6*- and
280 *FCGR3A*-expressing macrophages (Supplementary Figure 2C,D).
281
282 **T cell signature genes are downregulated in PECs from patients with LC CP-C**
283 We have also searched genes, expression of which is upregulated at CP-B and then
284 downregulated at CP-C. Expression of 126 genes were more than 2-fold upregulated in PECs
285 from patients with LC CP-B, compared with PECs from patients with LC CP-C and PECs from
286 patients undergoing CAPD (Fig.6 A,B). KEGG pathway analysis of these 126 genes
287 showed 'Natural killer cell mediated cytotoxicity' pathway was enriched with significance
288 (Fig.6B, C). Expression of *GZMB*, *IFNG*, *SH2D1A* and *LCK* in the pathway was elevated in
289 PECs from patients with LC CP-B. According to scRNA-seq analysis, these four genes were
290 highly expressed in T cells (Supplementary Figure 3A,B). These results suggest that T cells
291 increased in PECs from patients with LC CP-B, and then decreased in PECs from patients with
292 LC CP-C.
293
294 **Decrease of CD1c^{high} CD14^{int} DCs and increase of CD8α^{+} MAIT cells in LC patient-derived**

295 **PECs**

296 We analyzed surface expression of several lineage markers in PECs. $CD45^{+}$ cells of PECs are
297 shown as the CD1c versus CD14 profile (Fig.7A). This profile showed three major clusters,
298 $CD1c^{high}$ $CD14^{int}$ cells, $CD1c^{int}$ $CD14^{high}$ cells, and $CD1c^{low\text{-}int}$ $CD14^{low}$ cells. According to high
299 expression of CD1c, $CD1c^{high}$ $CD14^{int}$ cells can be regarded as DCs. $CD1c^{int}$ $CD14^{high}$ cells can
300 be regarded as *FCGR3A*-expressing macrophages, because they express CD16 but not CD1c
301 (Fig. 7D). Meanwhile, $CD1c^{low\text{-}int}$ $CD14^{low}$ cells are heterogenous and T cells were a major
302 population of them. Notably, quantitative real-time PCR analysis among fractions of $CD45^{+}$
303 PECs revealed that expression of *GATA6* was found only in $CD1c^{low\text{-}int}$ $CD14^{low}$ cells (Fig. 7B),
304 indicating that *GATA6*-expressing macrophages are contained in $CD1c^{low\text{-}int}$ $CD14^{low}$ cells.
305 According to the scRNA-seq analysis, it can be assumed that CD9 expression can be used to
306 identify *GATA6*-expressing macrophages. Then, we have examined surface CD9 expression in
307 $CD1c^{low\text{-}int}$ $CD14^{low}$ cells in CAPD or LC patient-derived PECs. The frequency of $CD1c^{low\text{-}int}$
308 $CD14^{low}$ $CD9^{+}$ cells was decreased in LC patient-derived PECs (Fig.7C).

309 Then we have examined the fluctuation of immune cell populations in LC patient-derived
310 PECs. $CD1c^{high}$ $CD14^{int}$ cells, that is, DCs were present in CAPD patient-derived PECs, while
311 they were decreased or absent in LC patient-derived PECs (Fig.7D). $CD1c^{int}$ $CD14^{high}$ cells were
312 decreased in LC patient-derived PECs compared with in CAPD patient-derived PECs. We have
313 then analyzed expression of CD16 and CD163 in $CD1c^{int}$ $CD14^{high}$ cells (Fig. 7E). Expression of
314 CD16 as well as CD163 was higher in LC patient-derived PECs than in CAPD patient-derived
315 PECs. Meanwhile, expression of CD16 and CD163 on DCs and $CD1c^{low\text{-}int}$ $CD14^{low}$ cells
316 remained low in LC patient-derived PECs. Thus, expression of CD16 and CD163 was elevated
317 only in $CD1c^{int}$ $CD14^{high}$ cells among LC patient-derived PECs. In patients with LC CP-B, T

318 cells including CD161^{+} TCR Vα7.2^{+} MAIT cells were increased (Fig.7F). These results were
319 consistent with both scRNA-seq analysis and bulk RNA-seq analysis.
320
321 **DISCUSSION**
322 The current study is the first report on comparative analysis to characterize immune cell
323 profiles of PECs between patients with LC and patients undergoing CAPD. Five main cell
324 clusters, including T cells, B cells, DCs and *GATA6*- and *FCGR3A*-expressing macrophages,
325 were found in PECs. In CAPD patient-derived PECs, DCs and *GATA6*- and *FCGR3A*-
326 expressing macrophages were dominant cell populations. This immune cell profile is consistent
327 with previous reports.[11,12] Meanwhile, in LC patient-derived PECs, DCs and two clusters of
328 macrophages decreased and T cells became dominant. Among DCs and macrophages, *FCGR3A*-
329 expressing macrophages were dominant in LC patient-derived PECs. Bulk RNA-seq analysis
330 further clarified up- or down-regulated gene lists between PECs from patients with LC and
331 those from patients undergoing CAPD. The results were consistent with scRNA-seq analysis of
332 PECs.
333 *FCGR3A*-expressing macrophages express *CD163*, *MARCO* and *LYVE1* and represent M2
334 type and anti-inflammatory phenotype. Meanwhile, DCs, which express *CD1C* and *CD1E*,
335 show M1 type and proinflammatory phenotype. Therefore, LC PECs tend to be skewed to M2.
336 In the liver, MAIT cells can promote liver fibrosis through the recruitment of profibrotic
337 monocytes.[14] In this context, increase of MAIT cells in the peritoneal cavity might cause
338 recruitment of *FCGR3A*-expressing macrophages. It should be intriguing to clarify the roles of
339 such recruited *FCGR3A*-expressing macrophages in progression of liver fibrosis.
340 *GATA6*-expressing macrophages are resident in the peritoneal cavity and also profibrotic, as
341 they express collagen gene such as *COL1A1* and repair-related genes (*THBS1*, *TGFB2*) (Fig.2A-

F). *GATA6*-expressing macrophages represent a minor population in LC patient-derived PECs. However, it is still possible that such macrophages migrate to the liver and provoke fibrosis, because *GATA6*-expressing macrophages in the peritoneal cavity are required for liver protection in murine liver injury model.[3]

We have further characterized gene expressions with LC severity. Compared with PECs from patients undergoing CAPD, expression of six genes was decreased in PECs from patients with LC CP-B and their expression levels were further reduced in PECs from patients with LC CP-C. Those genes were expressed mainly in DCs and *GATA6*-expressing macrophages. Among those genes, *CTLA4* encodes CTLA4, which can inhibit T cell proliferation.[15] *C15orf48* encodes modulator of cytochrome C oxidase during inflammation, which is a mitochondrial protein critically involved in autophagy induction and *C15orf48*-deficient mice showed development of autoimmunity, indicating that *C15orf48* regulates immune functions.[16] Decreased expression of these immunosuppressive molecules might perturb peritoneal immune homeostasis in patients with LC.

Meanwhile, four genes (*IDH1*, *CMKLR1*, *SLC7A8* and *SLC46A*) were found to increase in their expression as the LC stage progresses. Those genes were highly expressed in *GATA6*- and *FCGR3A*-expressing macrophages. *IDH1* encodes IDH, which generates α-ketoglutarate from isocitrate, thereby promoting differentiation of macrophages towards M2.[17,18] Expression of *CMKLR1* is high in macrophages from broncho alveolar lavages of patients with cystic fibrosis, indicating involvement of *CMKLR1* in fibrosis.[19] Expression of *SLC7A8* is also correlated with that of CD163 in M2 macrophages.[20] Thus, elevated expression of these genes might be related to upregulation of fibrotic or M2 type macrophage functions. It should be interesting whether or how those gene products contribute to progression of liver fibrosis.

365 Expression of some genes was elevated in PECs from patients with LC CP-B, but decreased in
366 PECs from patients with LC CP-C. KEGG pathway analysis of such gene enrichment of the
367 'Natural killer cell mediated cytotoxicity' pathway was enriched (Fig. 6C). This enrichment can
368 be assumed to be due to increase of T cells (Supplementary Figure 3A,B). Especially cytotoxic
369 T cell signature genes, *GZMB* and *IFNG,* were prominently elevated. MAIT cells, which are
370 also cytotoxic, are decreased in peripheral bloods, but increased in PECs from patients with
371 decompensated LC and spontaneous bacterial peritonitis (SBP).[2,21] In that study, patients with
372 LC were not categorized by CP classification. Meanwhile, we studied patients with LC at CP-B
373 and CP-C in the absence of SBP (Supplementary Table S1). It is interesting to elucidate how T
374 cells including MAIT cells are increased at CP-B and then decreased at CP-C. $CD163^{high}$ M2
375 type macrophages can inhibit T cell proliferation.[22] Therefore, the T cell decrease can be
376 ascribed to dominancy of M2 macrophages at CP-C. It is also possible that activated T cells
377 leave the peritoneal cavity and migrate to the liver.
378 FACS analysis showed that, in LC patient-derived PECs, $CD1c^{high}$ $CD14^{int}$ DCs were
379 decreased, while $CD16^{high}$ $CD163^{high}$ cells were increased (Fig. 7D,E). We further found that
380 $CD1^{low\text{-}int}$ $CD14^{low}$ cells include *GATA6*-expressing macrophages (Fig. 7B) and that these cells
381 were decreased in LC patient-derived PECs. Furthermore, T cells including MAIT cells were
382 increased and existed as a major population in LC patient-derived PECs. These flowcytometry
383 analysis results were consistent with the results of scRNA-seq and bulk RNA-seq analyses.
384 We thus characterized immune cell profiles of PECs from patients with LC. Whereas DCs and
385 macrophages were dominant in PECs from patients undergoing CAPD, T cells were the main
386 population in PECs from patients with LC. Although DCs and macrophages were decreased in
387 PECs from patients with LC, *FCGR3A*-expressing macrophages, which are profibrotic, were
388 relatively dominant over DCs and *GATA6*-expressing macrophages. We also compared gene

389 expression profiles between CP-B and CP-C and clarified that T cells were increased at CP-B
390 but decreased at CP-C. We further identified a set of genes expression of which was increased or
391 decreased with LC severity. Our present findings should have a potential to lead to further
392 development of diagnosis or therapeutic maneuver for LC.
393

394 **ACKNOWLEDGEMENTS**

395 We thank Ms. Sumiko Okura and Ms. Aoi Matsumura-Tawaki for secretarial assistance. We
396 acknowledge proofreading and editing by Benjamin Phillis at the Clinical Study Support Center,
397 Wakayama Medical University.
398

399 **REFERENCES**

400 1. GBD 2017 Cirrhosis Collaborators. The global, regional, and national burden of
401 cirrhosis by cause in 195 countries and territories, 1990-2017: a systematic analysis for the Global
402 Burden of Disease Study 2017. *Lancet Gastroenterol Hepatol*. Mar 2020;5(3):245-266.
403 doi:10.1016/s2468-1253(19)30349-8
404 2. Niehaus CE, Strunz B, Cornillet M, et al. MAIT Cells Are Enriched and Highly
405 Functional in Ascites of Patients With Decompensated Liver Cirrhosis. *Hepatology*. Oct
406 2020;72(4):1378-1393. doi:10.1002/hep.31153
407 3. Wang J, Kubes P. A Reservoir of Mature Cavity Macrophages that Can Rapidly Invade
408 Visceral Organs to Affect Tissue Repair. *Cell*. Apr 21 2016;165(3):668-78.
409 doi:10.1016/j.cell.2016.03.009
410 4. Hossain M, Shim R, Lee WY, Sharpe AH, Kubes P. Gata6(+) resident peritoneal
411 macrophages promote the growth of liver metastasis. *Nat Commun*. Jul 29 2022;13(1):4406.
412 doi:10.1038/s41467-022-32080-y

413 5. Chang H, Ni Y, Shen C, et al. Peritoneal GATA6(+) macrophage drives hepatic
414 immunopathogenesis and maintains the T(reg) cell niche in the liver. *Immunology*. Sep
415 2022;167(1):77-93. doi:10.1111/imm.13519
416 6. Goedhart J, Luijsterburg MS. VolcaNoseR is a web app for creating, exploring, labeling
417 and sharing volcano plots. *Sci Rep*. Nov 25 2020;10(1):20560. doi:10.1038/s41598-020-76603-3
418 7. Chakarov S, Lim HY, Tan L, et al. Two distinct interstitial macrophage populations
419 coexist across tissues in specific subtissular niches. *Science*. Mar 15 2019;363(6432).
420 doi:10.1126/science.aau0964
421 8. Ghosn EE, Cassado AA, Govoni GR, et al. Two physically, functionally, and
422 developmentally distinct peritoneal macrophage subsets. *Proc Natl Acad Sci U S A*. Feb 9
423 2010;107(6):2568-2573. doi:10.1073/pnas.0915000107
424 9. Rosas M, Davies LC, Giles PJ, et al. The transcription factor Gata6 links tissue
425 macrophage phenotype and proliferative renewal. *Science*. May 9 2014;344(6184):645-648.
426 doi:10.1126/science.1251414
427 10. Okabe Y, Medzhitov R. Tissue-specific signals control reversible program of
428 localization and functional polarization of macrophages. *Cell*. May 8 2014;157(4):832-44.
429 doi:10.1016/j.cell.2014.04.016
430 11. Han J, Gallerand A, Erlich EC, et al. Human serous cavity macrophages and dendritic
431 cells possess counterparts in the mouse with a distinct distribution between species. *Nat Immunol*.
432 Jan 2024;25(1):155-165. doi:10.1038/s41590-023-01688-7
433 12. Hu W, Li G, Dong W, et al. Single-cell sequencing reveals peritoneal environment and
434 insights into fibrosis in CAPD patients. *iScience*. Apr 21 2023;26(4):106336.
435 doi:10.1016/j.isci.2023.106336
436 13. Durand F, Valla D. Assessment of the prognosis of cirrhosis: Child-Pugh versus MELD.

437 *J Hepatol*. 2005;42 Suppl(1):S100-7. doi:10.1016/j.jhep.2004.11.015

438 14. Mabire M, Hegde P, Hammoutene A, et al. MAIT cell inhibition promotes liver fibrosis
439 regression via macrophage phenotype reprogramming. *Nat Commun*. Apr 1 2023;14(1):1830.
440 doi:10.1038/s41467-023-37453-5

441 15. Laurent S, Carrega P, Saverino D, et al. CTLA-4 is expressed by human monocyte-
442 derived dendritic cells and regulates their functions. *Hum Immunol*. Oct 2010;71(10):934-41.
443 doi:10.1016/j.humimm.2010.07.007

444 16. Takakura Y, Machida M, Terada N, et al. Mitochondrial protein C15ORF48 is a stress-
445 independent inducer of autophagy that regulates oxidative stress and autoimmunity. *Nat Commun*.
446 Feb 1 2024;15(1):953. doi:10.1038/s41467-024-45206-1

447 17. Liu PS, Wang H, Li X, et al. α-ketoglutarate orchestrates macrophage activation through
448 metabolic and epigenetic reprogramming. *Nat Immunol*. Sep 2017;18(9):985-994.
449 doi:10.1038/ni.3796

450 18. Mouton AJ, Aitken NM, Moak SP, et al. Temporal changes in glucose metabolism reflect
451 polarization in resident and monocyte-derived macrophages after myocardial infarction. *Front*
452 *Cardiovasc Med*. 2023;10:1136252. doi:10.3389/fcvm.2023.1136252

453 19. Mannes PZ, Barnes CE, Biermann J, et al. Molecular imaging of chemokine-like
454 receptor 1 (CMKLR1) in experimental acute lung injury. *Proc Natl Acad Sci U S A*. Jan 17
455 2023;120(3):e2216458120. doi:10.1073/pnas.2216458120

456 20. Zhao X, Jin L, Liu Y, Liu Z, Liu Q. Bioinformatic analysis of the role of solute carrier-
457 glutamine transporters in breast cancer. *Ann Transl Med*. Jul 2022;10(14):777. doi:10.21037/atm-
458 22-2620

459 21. Ibidapo-Obe O, Stengel S, Köse-Vogel N, et al. Mucosal-Associated Invariant T Cells
460 Redistribute to the Peritoneal Cavity During Spontaneous Bacterial Peritonitis and Contribute to

461 Peritoneal Inflammation. *Cell Mol Gastroenterol Hepatol*. 2020;9(4):661-677.
462 doi:10.1016/j.jcmgh.2020.01.003
463 22. Han Q, Shi H, Liu F. CD163(+) M2-type tumor-associated macrophage support the
464 suppression of tumor-infiltrating T cells in osteosarcoma. *Int Immunopharmacol*. May
465 2016;34:101-106. doi:10.1016/j.intimp.2016.01.023
466
467

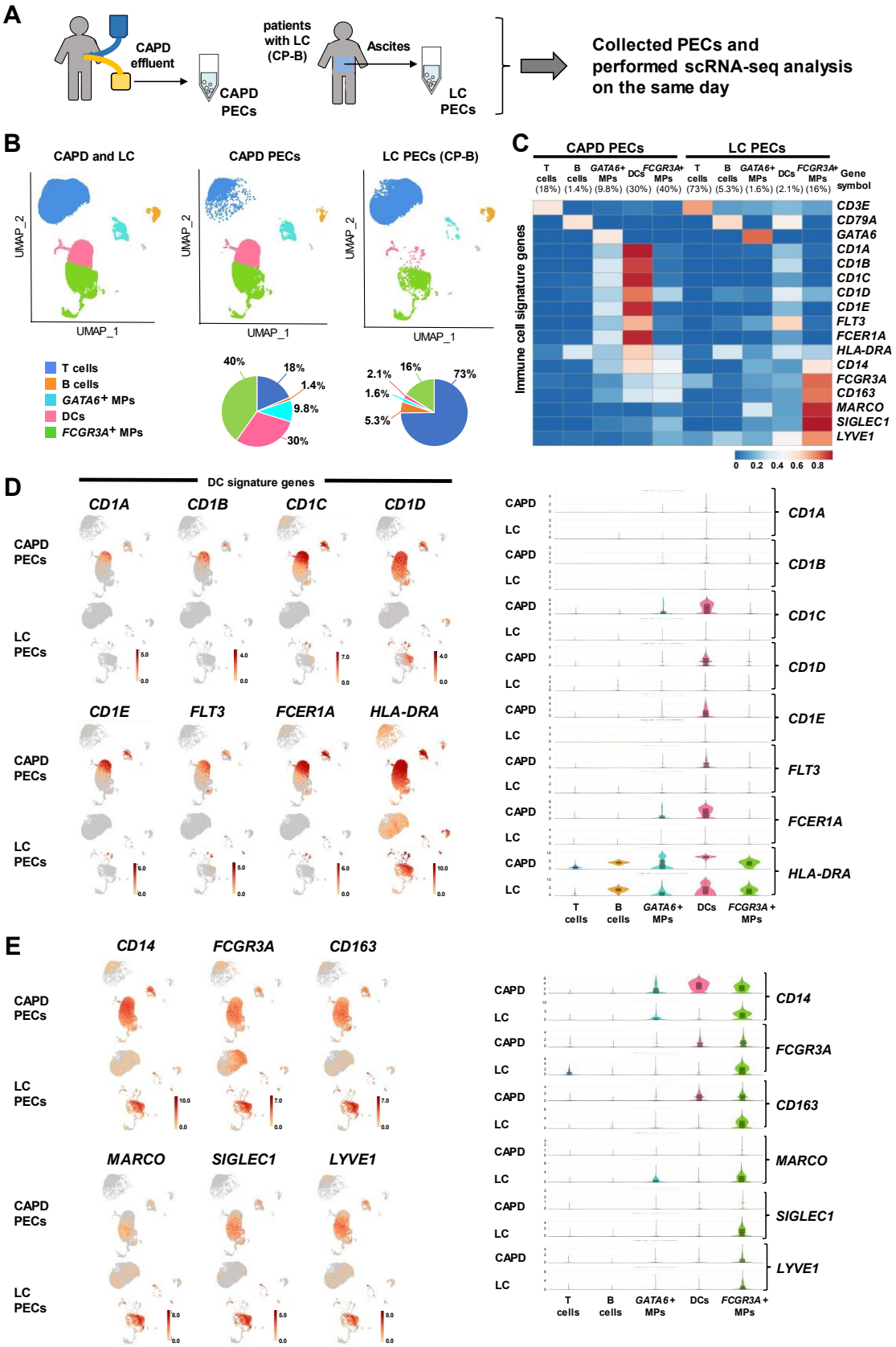
A
CAPD effluent
CAPD PECs
patients with LC (CP-B)
Ascites
LC PECs
Collected PECs and performed scRNA-seq analysis on the same day
B
CAPD and LC
CAPD PECs
LC PECs (CP-B)
UMAP_2
UMAP_1
T cells
B cells
GATA6+ MPs
DCs
FCGR3A+ MPs
40%
18%
1.4%
9.8%
30%
2.1%
16%
73%
1.6%
5.3%
C
CAPD PECs
LC PECs
T cells (18%)
B cells (1.4%)
GATA6+ MPs (9.8%)
DCs (30%)
FCGR3A+ MPs (40%)
T cells (73%)
B cells (5.3%)
GATA6+ MPs (1.6%)
DCs (2.1%)
FCGR3A+ MPs (16%)
Gene symbol
Immune cell signature genes
CD3E
CD79A
GATA6
CD1A
CD1B
CD1C
CD1D
CD1E
FLT3
FCER1A
HLA-DRA
CD14
FCGR3A
CD163
MARCO
SIGLEC1
LYVE1
0 0.2 0.4 0.6 0.8
D
DC signature genes
CD1A
CD1B
CD1C
CD1D
CD1E
FLT3
FCER1A
HLA-DRA
CAPD PECs
LC PECs
CAPD
LC
T cells
B cells
GATA6+ MPs
DCs
FCGR3A+ MPs
E
CD14
FCGR3A
CD163
MARCO
SIGLEC1
LYVE1
CAPD PECs
LC PECs
CAPD
LC
T cells
B cells
GATA6+ MPs
DCs
FCGR3A+ MPs

468

469 **FIG.1. Single-cell RNA sequencing analysis revealed major cell clusters and gene expression**
470 **profiles of CAPD and LC patient-derived PECs**
471 (A) Schematic workflow of scRNA-seq analysis of human PECs.
472 (B) UMAP shows five distinct clusters of CAPD PECs (CAPD patient-derived PECs) and LC
473 PECs (LC patient-derived PECs). Clusters include T cells, B cells, *GATA6*-expressing
474 macrophages (*GATA6*$^{+}$ MPs), DCs and *FCGR3A*-expressing macrophages (*FCGR3A*$^{+}$ MPs).
475 (C) Heatmap shows five clusters of CAPD and LC PECs and the expression of immune cell
476 signature genes.
477 (D) Feature plots and violin plots of DC signature gene expression in CAPD and LC PECs.
478 (E) Feature plots or violin plots of expression of *CD14*, *FCGR3A*, *CD163*, *MARCO*, *SIGLEC1*
479 and *LYVE1* in CAPD and LC PECs.
480
481

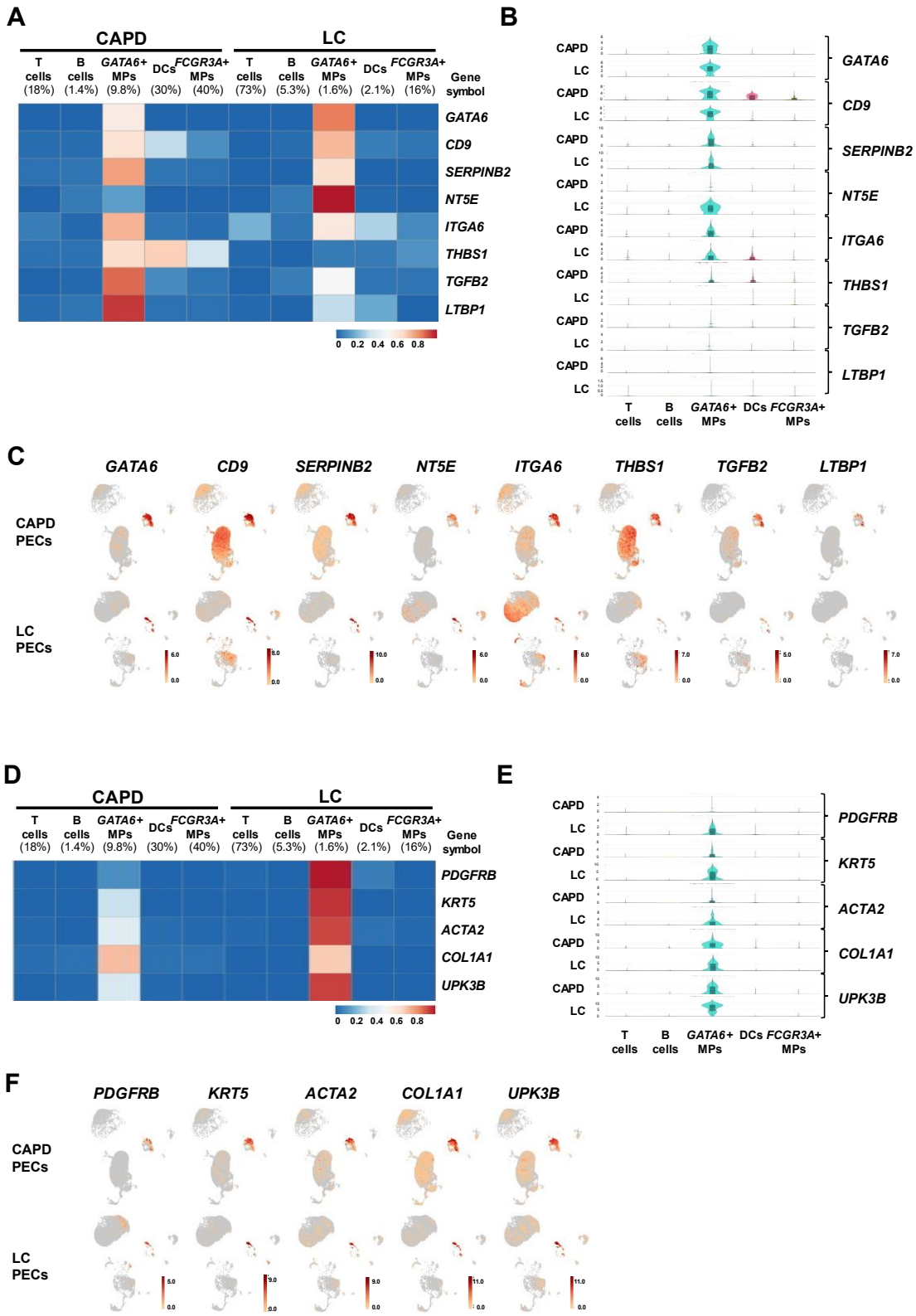
A
CAPD
LC
T cells (18%)
B cells (1.4%)
GATA6+ MPs (9.8%)
DCs (30%)
FCGR3A+ MPs (40%)
T cells (73%)
B cells (5.3%)
GATA6+ MPs (1.6%)
DCs (2.1%)
FCGR3A+ MPs (16%)
Gene symbol
GATA6
CD9
SERPINB2
NT5E
ITGA6
THBS1
TGFB2
LTBP1
0 0.2 0.4 0.6 0.8
B
CAPD
LC
T cells
B cells
GATA6+ MPs
DCs
FCGR3A+ MPs
C
GATA6
CD9
SERPINB2
NT5E
ITGA6
THBS1
TGFB2
LTBP1
CAPD PECs
LC PECs
D
PDGFRB
KRT5
ACTA2
COL1A1
UPK3B
E
F

482

483 **FIG.2. Single-cell RNA sequencing analysis revealed gene expression profiles of *GATA6*-**
484 **expressing macrophages in CAPD and LC patient-derived PECs**

485 (A-C) Gene expression of *GATA6*, *CD9*, *SERPINB2*, *NT5E*, *ITGA6*, *THBS1*, *TGFB2* and *LTBP1*
486 is shown in heatmap (A), violin plots (B) and feature plots (C).

487 (D-F) Gene expression of *PDGFRB*, *KRT5*, *ACTA2*, *COL1A1* and *UPK3B* is shown in heatmap
488 (D), violin plots (E) and feature plots (F).

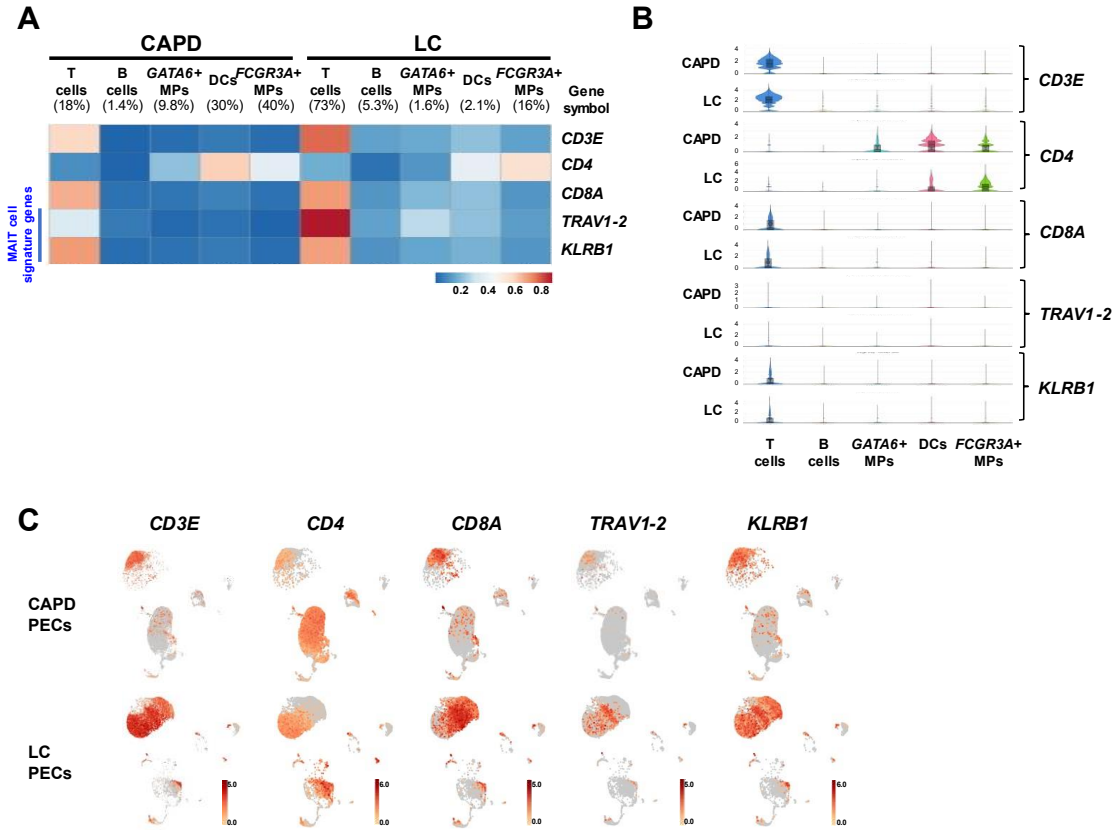

FIG.3. Single-cell RNA sequencing analysis revealed gene expression profiles of T cells in CAPD and LC patient-derived PECs

(A-C) Gene expression of *CD3E*, *CD4*, *CD8A*, *TRAV1-2* and *KLRB1* is shown in heatmap (A), violin plots (B) and feature plots (C).

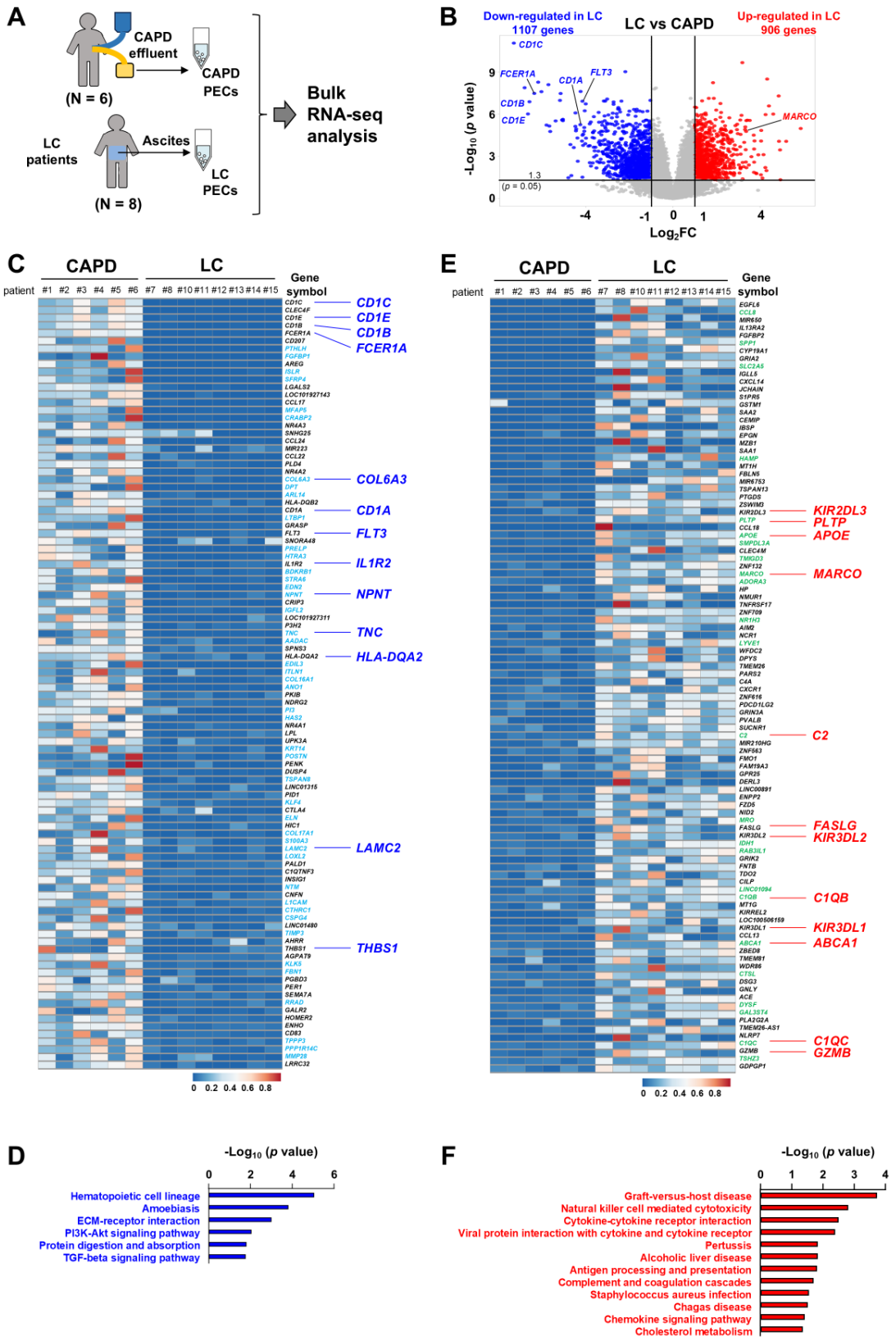
A
CAPD effluent
CAPD PECs
(N = 6)
LC patients
Ascites
LC PECs
(N = 8)
Bulk RNA-seq analysis
B
Down-regulated in LC
1107 genes
LC vs CAPD
Up-regulated in LC
906 genes
CD1C
FCER1A
CD1A
FLT3
CD1B
CD1E
MARCO
-Log10 (p value)
(p = 0.05)
Log2FC
C
CAPD
LC
patient
Gene symbol
CD1C
CD1E
CD1B
FCER1A
COL6A3
CD1A
FLT3
IL1R2
NPNT
TNC
HLA-DQA2
LAMC2
THBS1
E
KIR2DL3
PLTP
APOE
MARCO
C2
FASLG
KIR3DL2
C1QB
KIR3DL1
ABCA1
C1QC
GZMB
D
-Log10 (p value)
Hematopoietic cell lineage
Amoebiasis
ECM-receptor interaction
PI3K-Akt signaling pathway
Protein digestion and absorption
TGF-beta signaling pathway
F
-Log10 (p value)
Graft-versus-host disease
Natural killer cell mediated cytotoxicity
Cytokine-cytokine receptor interaction
Viral protein interaction with cytokine and cytokine receptor
Pertussis
Alcoholic liver disease
Antigen processing and presentation
Complement and coagulation cascades
Staphylococcus aureus infection
Chagas disease
Chemokine signaling pathway
Cholesterol metabolism

495

496 **FIG.4. Bulk RNA sequencing analysis revealed that DCs and *GATA6*-expressing**
497 **macrophages mainly decreased in LC patient-derived PECs**

498 (A) Schematic workflow of bulk RNA-seq analysis of human PECs.

499 (B) Volcano plots of gene expression in PECs show a fold change (FC) and *p* value for the
500 comparison of LC PECs versus CAPD PECs. Up- or down- regulated genes (FC ≥ 2, $p <$
501 0.05) are depicted in red or blue, respectively.

502 (C) Heatmap of the top 100 downregulated genes in LC PECs.

503 (D) KEGG pathway analysis of downregulated genes in (C).

504 (E) Heatmap of the top 100 upregulated genes in LC PECs.

505 (F) KEGG pathway analysis of upregulated genes in (E).

506

507

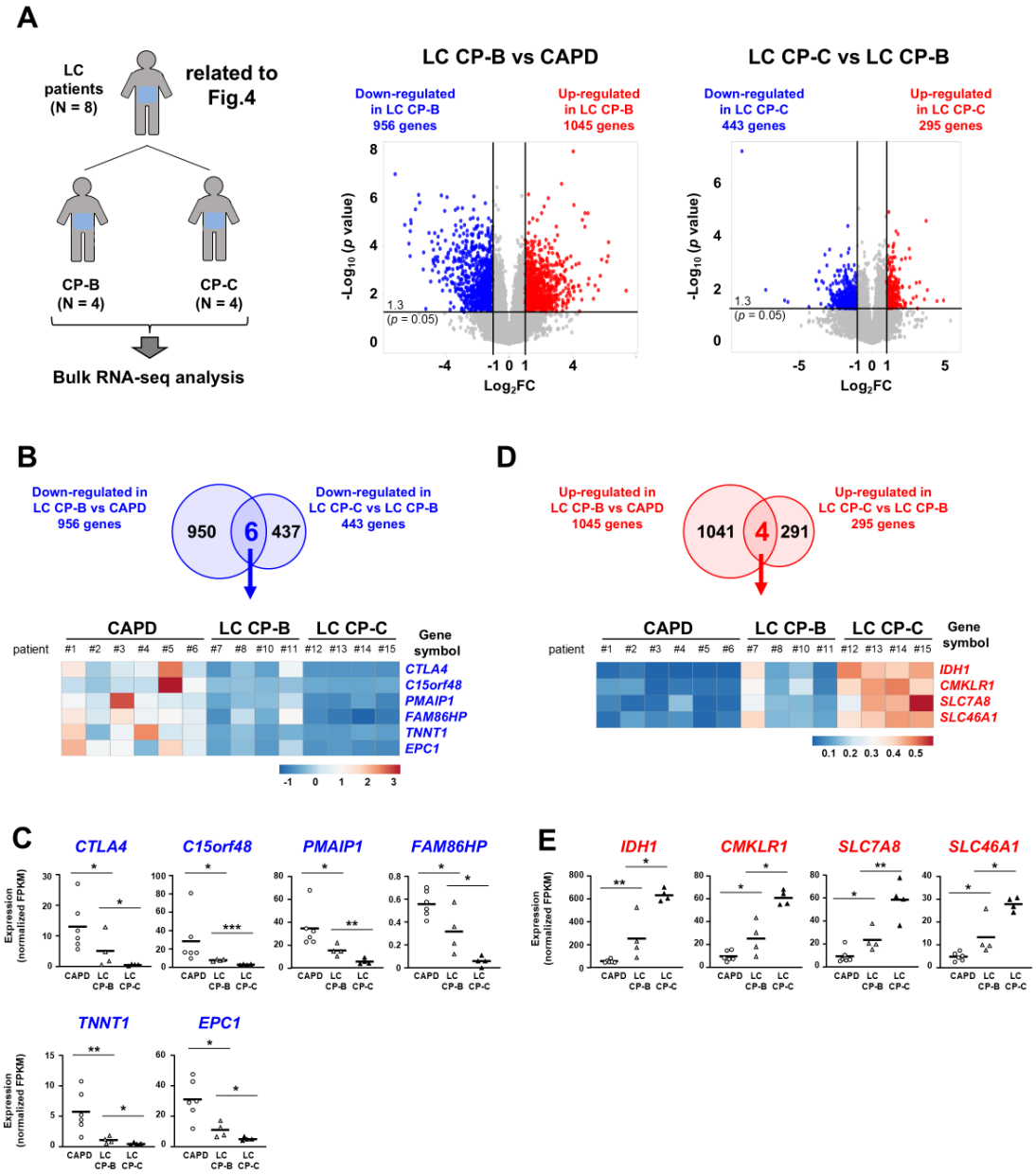

508

509 **FIG.5. Bulk RNA sequencing analysis revealed up- or down- regulated genes in correlation**

510 **with LC severity**

511 (A) Volcano plots of gene expression show a FC and *p* value for the comparisons of LC CP-B

512 PECs versus CAPD PECs (middle) or LC CP-C PECs versus LC CP-B PECs (right). Two-

513 fold up- or down- regulated genes (FC ≥ 2, $p < 0.05$) with significance are depicted in red or

514 blue, respectively.

(B) Venn diagram depicting the numbers of 2-fold downregulated genes with significance in LC CP-B PECs (A, middle) or LC CP-C PECs (A, right), then expression of the overlapped six genes showed in heatmap.

(C) Expression of the six genes (B). Statistical significance was determined by an unpaired two-tailed Student's t test. *p* values are indicated by $*p < 0.05$, $**p < 0.01$. $p < 0.05$ was considered statistically significant.

(D) Venn diagram depicting the numbers of 2-fold upregulated genes with significance in LC CP-B PECs (A, middle) or LC CP-C PECs (A, right), then expression of the overlapped four genes showed in heatmap.

(E) Expression of the four genes (D). Statistical significance was determined by an unpaired two-tailed Student's t test. *p* values are indicated by $*p < 0.05$, $**p < 0.01$. $p < 0.05$ was considered statistically significant.

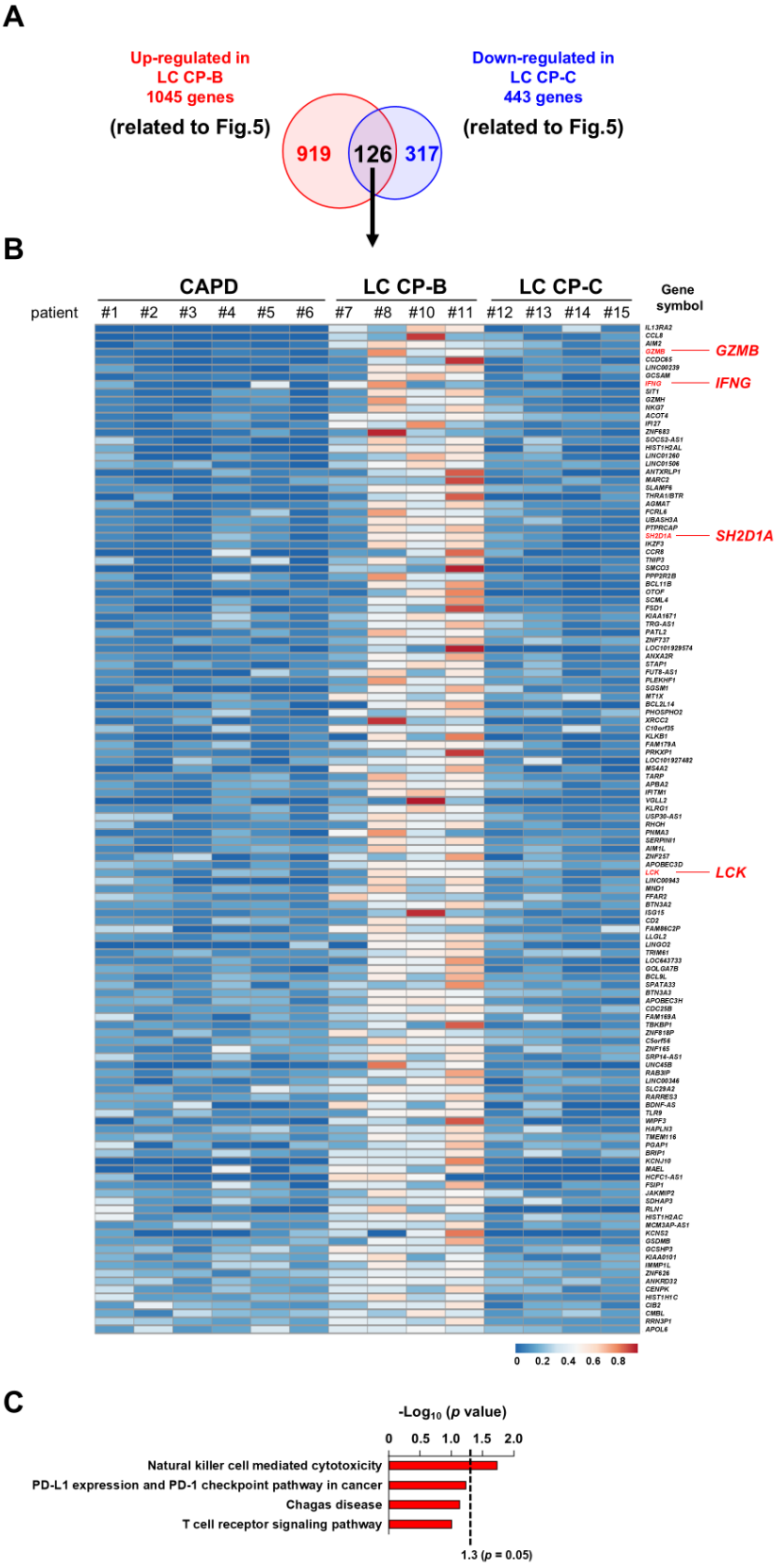
A
Up-regulated in
LC CP-B
1045 genes
(related to Fig.5)
919
126
317
Down-regulated in
LC CP-C
443 genes
(related to Fig.5)
B
CAPD
LC CP-B
LC CP-C
patient
#1 #2 #3 #4 #5 #6 #7 #8 #10 #11 #12 #13 #14 #15
Gene symbol
GZMB
IFNG
SH2D1A
LCK
0 0.2 0.4 0.6 0.8
C
-Log10 (p value)
0 0.5 1.0 1.5 2.0
Natural killer cell mediated cytotoxicity
PD-L1 expression and PD-1 checkpoint pathway in cancer
Chagas disease
T cell receptor signaling pathway
1.3 (p = 0.05)

529

530 **FIG.6. Bulk RNA sequencing analysis revealed that T cell signature genes were upregulated**

531 **in LC CP-B but not LC CP-C**

532 (A) Venn diagram depicting the numbers of upregulated genes in LC CP-B (Fig.5A, middle) or

533 those of downregulated genes in LC CP-C (Fig.5A, right).

534 (B) Heatmap of overlapped genes in (A).

535 (C) KEGG pathway analysis of overlapped genes in (A).

536

537

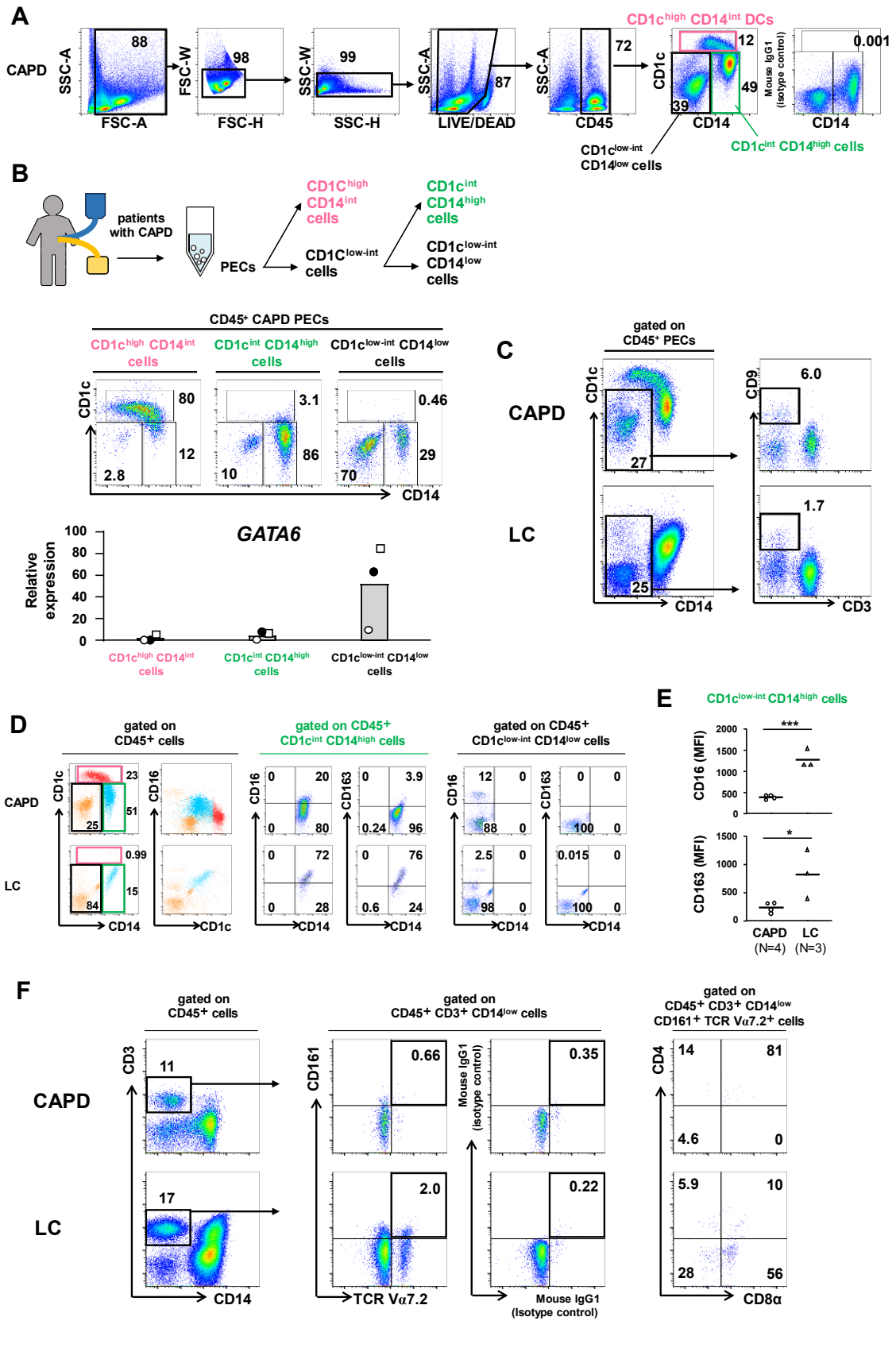
A
CAPD
SSC-A
FSC-A
88
FSC-W
FSC-H
98
SSC-W
SSC-H
99
SSC-A
LIVE/DEAD
87
SSC-A
CD45
72
CD1c
CD14
12
49
39
CD1c^high CD14^int DCs
CD1c^low-int CD14^low cells
CD1c^int CD14^high cells
Mouse IgG1 (isotype control)
CD14
0.001
B
patients with CAPD
PECs
CD1C^high CD14^int cells
CD1C^low-int cells
CD1c^int CD14^high cells
CD1c^low-int CD14^low cells
CD45+ CAPD PECs
CD1c^high CD14^int cells
CD1c^int CD14^high cells
CD1c^low-int CD14^low cells
CD1c
CD14
80
12
2.8
3.1
86
10
0.46
29
70
GATA6
Relative expression
100
80
60
40
20
0
C
gated on CD45+ PECs
CAPD
LC
CD1c
CD14
27
25
CD9
CD3
6.0
1.7
D
gated on CD45+ cells
gated on CD45+ CD1c^int CD14^high cells
gated on CD45+ CD1c^low-int CD14^low cells
CAPD
LC
CD1c
CD16
CD163
CD14
23
51
25
0.99
15
84
0
20
80
72
28
3.9
96
76
24
12
88
2.5
98
0.015
100
E
CD1c^low-int CD14^high cells
CD16 (MFI)
CD163 (MFI)
2000
1500
1000
500
0
***
*
CAPD (N=4)
LC (N=3)
F
gated on CD45+ cells
gated on CD45+ CD3+ CD14^low cells
gated on CD45+ CD3+ CD14^low CD161+ TCR Vα7.2+ cells
CAPD
LC
CD3
CD14
11
17
CD161
TCR Vα7.2
0.66
2.0
Mouse IgG1 (isotype control)
0.35
0.22
CD4
CD8α
14
81
4.6
0
5.9
10
28
56

538

539 **FIG.7. Flowcytometry analysis revealed decrease of DCs and increase of CD16^{high} CD163^{high}**

540 **macrophages and CD8α^{+} MAIT cells in LC PECs**

541 (A) Gating strategy to identify CD1c^{high} CD14^{int}, CD1c^{int} CD14^{high} and CD1c$^{low\text{-}int}$ CD14^{low} cells

542 in CAPD PECs. Numbers indicate percentages of gated cells.

543 (B) CD1c^{high} CD14^{int}, CD1c^{int} CD14^{high} and CD1c$^{low\text{-}int}$ CD14^{low} cells were purified from CAPD

544 PECs by MACS system. Expression of *GATA6* among these three subsets is shown (N=3).

545 (C) Frequency of CD1c$^{low\text{-}int}$ CD14^{low} CD9^{+} cells in CAPD PECs and LC PECs. Numbers

546 indicate percentages of gated cells.

547 (D) Surface expression of CD1c, CD14, CD16 and CD163 in CD1c^{high} CD14^{int}, CD1c^{int}

548 CD14^{high} and CD1c$^{low\text{-}int}$ CD14^{low} cells in CAPD PECs or LC PECs. Red dots indicate

549 CD1c^{high} CD14^{int} cells, blue dots indicate CD1c^{int} CD14^{high} cells and orange dots indicate

550 CD1c$^{low\text{-}int}$ CD14^{low} cells, respectively. Numbers indicate percentages of gated cells.

551 (E) Surface expression of CD16 and CD163 in CD1c$^{low\text{-}int}$ CD14^{high} cells in CAPD PECs (N=4)

552 or LC PECs (N=3). MFI indicates mean fluorescence intensity. Statistical significance was

553 determined by an unpaired two-tailed Student's t test. p values are indicated by *$p < 0.05$,

554 ***$p < 0.001$. $p < 0.05$ was considered statistically significant.

555 (F) Surface expression of T cell markers in CAPD PECs or LC PECs. Numbers indicate

556 percentage of gated cells.

557

558

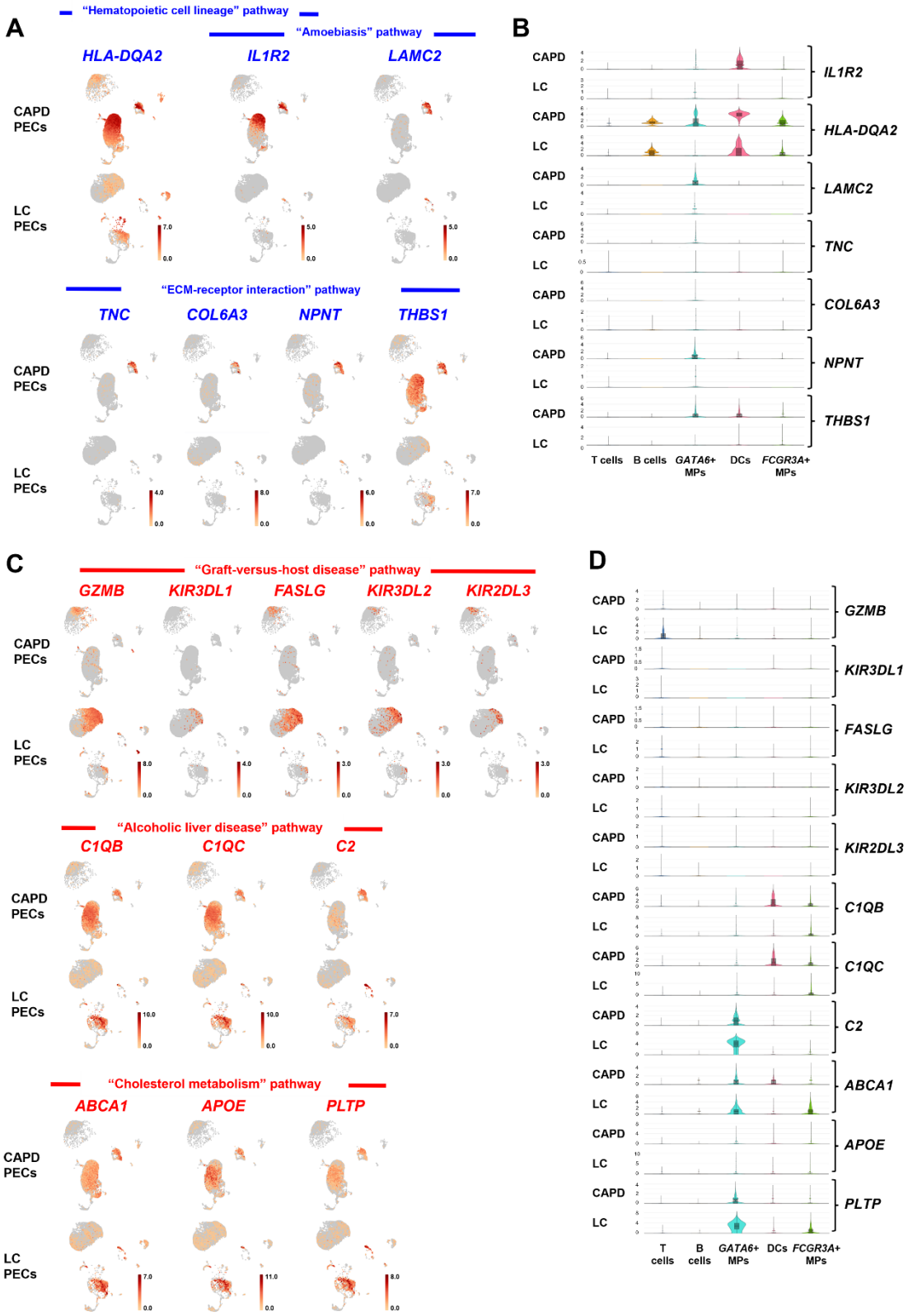
A
"Hematopoietic cell lineage" pathway
"Amoebiasis" pathway
HLA-DQA2
IL1R2
LAMC2
CAPD PECs
LC PECs
"ECM-receptor interaction" pathway
TNC
COL6A3
NPNT
THBS1
B
CAPD
LC
IL1R2
HLA-DQA2
LAMC2
TNC
COL6A3
NPNT
THBS1
T cells
B cells
GATA6+ MPs
DCs
FCGR3A+ MPs
C
"Graft-versus-host disease" pathway
GZMB
KIR3DL1
FASLG
KIR3DL2
KIR2DL3
"Alcoholic liver disease" pathway
C1QB
C1QC
C2
"Cholesterol metabolism" pathway
ABCA1
APOE
PLTP
D
T cells
B cells
GATA6+ MPs
DCs
FCGR3A+ MPs

559

560 **Supplementary Figure 1**

561 **Gene expression profiles of up- or down- regulated genes in LC patient-derived PECs by**

562 **scRNA-seq analysis**

563 (A,B) Expression of *HLA-DQA2*, *IL1R2*, *LAMC2*, *TNC*, *COL6A3*, *NPNT* and *THBS1* is shown in

564 feature plots (A) and violin plots (B).

565 (C,D) Expression of *GZMB*, *KIR3DL1*, *FASLG*, *KIR3DL2*, *KIR2DL3*, *C1QB*, *C1QC*, *C2*, *ABCA1*,

566 *APOE* and *PLTP* is shown in feature plots (C) and violin plots (D).

567

568

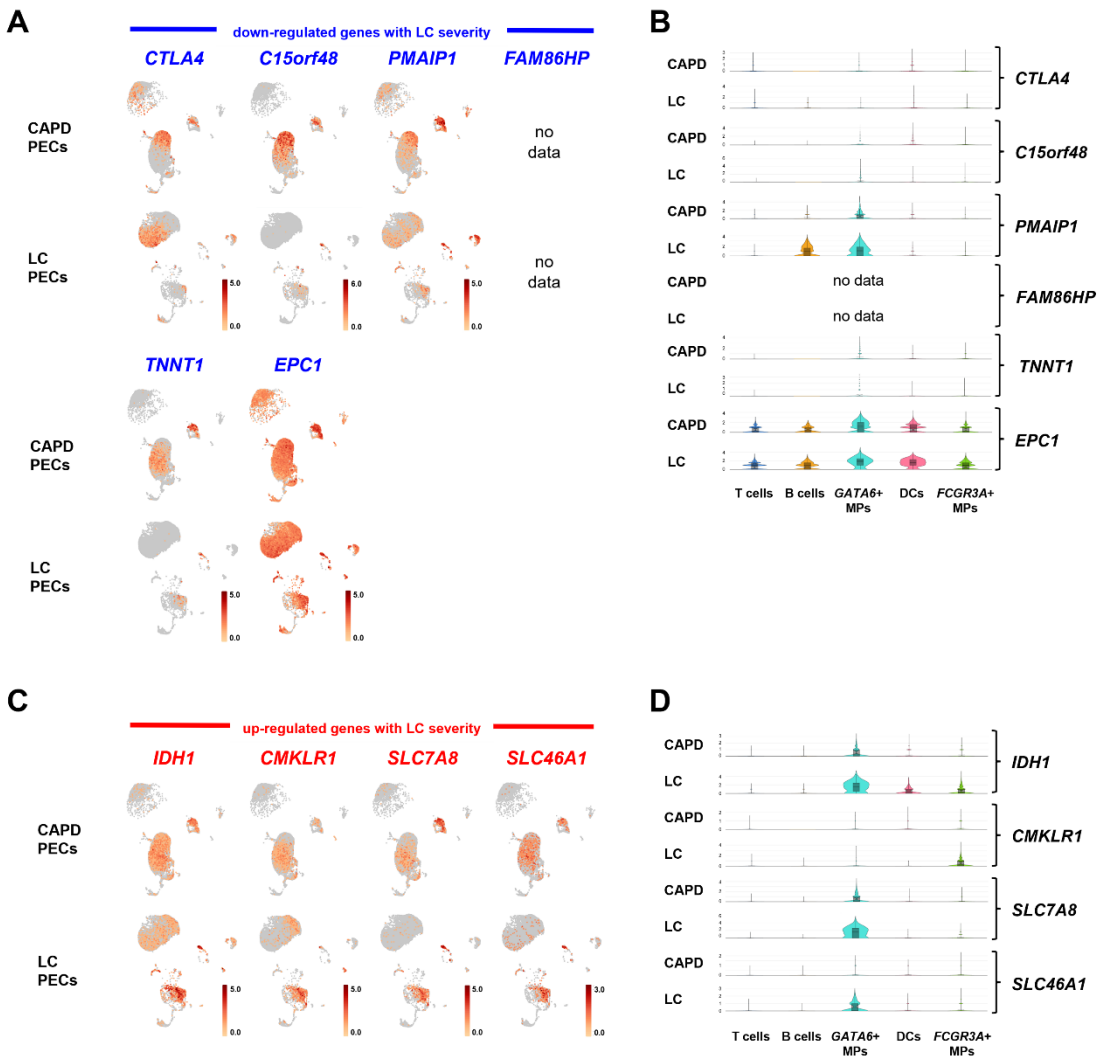

Supplementary Figure 2

Gene expression profiles of up- or down- regulated genes with LC severity by scRNA-seq analysis

(A,B) Expression of *CTLA4*, *C15orf48*, *PMAIP1*, *FAM86HP*, *TNNT1* and *EPC1* is shown in feature plots (A) and violin plots (B).

(C,D) Expression of *IDH1*, *CMKLR1*, *SLC7A8* and *SLC46A1* is shown in feature plots (C) and violin plots (D).

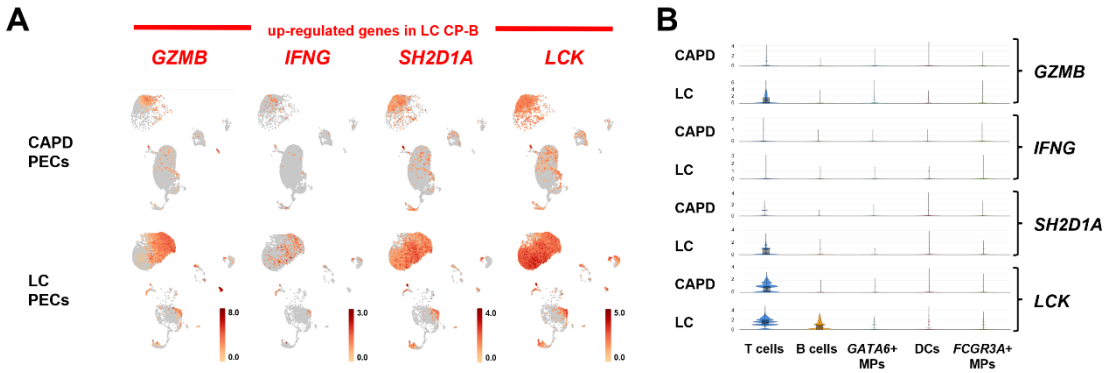

Supplementary Figure 3

Gene expression profiles of upregulated genes in LC CP-B patient-derived PECs by scRNA-seq analysis

(A,B) Expression of *GZMB*, *IFNG*, *SH2D1A* and *LCK* is shown in feature plots (A) and violin plots (B).

586 **Supplementary Table S1.** Patients undergoing CAPD or with LC enrolled in this study

Patient	Group	Etiology of LC	Experiment performed	SBP
#1	CAPD	-	sample 1 ; Bulk RNA-seq sample 2 ; scRNA-seq sample 3 ; Flowcytometry	not tested
#2	CAPD	-	sample 1 ; Bulk RNA-seq sample 2 ; Flowcytometry	not tested
#3	CAPD	-	sample 1 ; Bulk RNA-seq sample 2, 3 ; Flowcytometry	not tested
#4	CAPD	-	Bulk RNA-seq	not tested
#5	CAPD	-	Bulk RNA-seq	not tested
#6	CAPD	-	Bulk RNA-seq	not tested
#7	LC CP-B	MASLD	Bulk RNA-seq, Flowcytometry	Negative
#8	LC CP-B	Hepatitis C	Bulk RNA-seq, Flowcytometry	Negative
#9	LC CP-B	PBC	Flowcytometry	Negative
#10	LC CP-B	ALD	Bulk RNA-seq, Flowcytometry	Negative
#11	LC CP-B	MASLD	sample 1 ; scRNA-seq, Bulk RNA-seq sample 2 ; Flowcytometry	Negative

#12	**LC CP-C**	**PSC+AIH**	**Bulk RNA-seq, Flowcytometry**	**Negative**
#13	**LC CP-C**	**postoperative cholangitis**	**Bulk RNA-seq, Flowcytometry**	**Negative**
#14	**LC CP-C**	**PSC**	**Bulk RNA-seq, Flowcytometry**	**Negative**
#15	**LC CP-C**	**ALD**	**Bulk RNA-seq**	**Negative**
#16	**CAPD**	**-**	**Flowcytometry**	**not tested**
#17	**LC CP-B**	**ALD**	**Flowcytometry**	**Negative**
#18	**LC CP-B**	**unknown**	**Flowcytometry**	**Negative**

Summary of each assay is shown.

SBP, spontaneous bacterial peritonitis; MASLD, metabolic dysfunction associated steatotic liver disease; PBC, primary biliary cholangitis; ALD, alcoholic liver disease; PSC, primary sclerosing cholangitis; AIH, autoimmune hepatitis

593 **Supplementary Table S2.** Clinical characteristics of the study individuals for scRNA-seq
594 analysis

	Analysis of scRNA-seq	
Characteristic	**CAPD (N = 1)**	**LC CP-B (N = 1)**
Age, y	**69**	**76**
Male sex	**Male**	**Male**
Serum leukocytes ($\times 10^9$/l)	**5.86**	**3.09**
Plt ($\times 10^9$ /l)	**248**	**52**
Serum PT (%)	**-**	**60.9**
Serum Albumin (g/dl)	**3.0**	**2.9**
AST (U/l)	**13**	**15**
ALT (U/l)	**13**	**11**
T-Bil (mg/dl)	**0.5**	**0.9**

595
596
597
598
599
600
601

602 **Supplementary Table S3.** Clinical characteristics of the study individuals for bulk RNA-seq

603 analysis

	Analysis of Bulk RNA-seq		
Characteristic	**CAPD (N = 6)**	**LC CP-B (N = 4)**	**LC CP-C (N = 4)**
Age, y	**63.5 (45-77)**	**74 (65-81)**	**59.5 (45-69)**
Sex (male / female)	**4 / 2**	**2 / 2**	**3 / 1**
Body Mass Index	**25.1 (21.3-32.5)**	**22.5 (17.9-33.0)**	**20.6 (19.0-20.9)**
Serum leukocytes ($\times 10^9$/l)	**5.445 (3.580-11.46)**	**4.280 (3.090-6.190)**	**7.980 (5.480-10.08)**
Plt ($\times 10^9$/l)	**203.5 (170-292)**	**54.5 (52-245)**	**111 (82-128)**
Serum PT (%)	**-**	**77.25 (60.9-87.9)**	**52.7 (49-66.1)**
Serum Albumin (g/dl)	**3.15 (2.9-3.6)**	**2.8 (2.6-2.9)**	**2.05 (2.0-2.8)**
AST (U/l)	**15.5 (11-22)**	**41 (15-65)**	**50.5 (30-454)**
ALT (U/l)	**14 (6-45)**	**13 (9-50)**	**35.5 (13-120)**
T-Bil (mg/dl)	**-**	**1.3 (0.5-1.7)**	**8.95 (0.7-23.4)**
Creatinine	**11.71 (9.33-12.04)**	**0.975 (0.82-1.17)**	**1.085 (0.52-4.16)**

604

605

606

607

608 **Supplementary Table S4.** Antibodies used for flowcytometry analysis

Antibody name	Color	Clone	Cat	Antibody source
anti-CD45	APC	HI30	304037	BioLegend
anti-CD1c	Biotin	L161	331504	BioLegend
anti-CD14	PE	61D3	12-0149-42	Invitrogen
anti-CD9	PerCPCy5.5	HI9A	312110	BioLegend
anti-CD3	APCCy7	UCTH1	300426	BioLegend
anti-CD16 (encoded by *FCGR3A*)	Pacific Blue	3G8	980106	BioLegend
anti-CD163	FITC	GHI/61	333617	BioLegend
anti- CD161	PECy7	HP-3G10	339918	BioLegend
anti-TCR Vα7.2	Brilliant violet 421	3C10	351716	BioLegend
anti-CD4	PerCPCy5.5	RPA-T4	300530	BioLegend
anti-CD8α	FITC	RPA-T8	301060	BioLegend

609